

## 12/10- and 11/13-Mixed Helices in $\alpha/\gamma$ - and $\beta/\gamma$ -Hybrid Peptides Containing C-Linked Carbo- $\gamma$ -amino Acids with Alternating $\alpha$ - and $\beta$ -Amino Acids

Gangavaram V. M. Sharma,<sup>\*,†</sup> Vivekanand B. Jadhav,<sup>†</sup>  
Kallaganti V. S. Ramakrishna,<sup>‡</sup> Pagadala Jayaprakash,<sup>†</sup> Kongari Narsimulu,<sup>‡</sup>  
Velaparthy Subash,<sup>†</sup> and Ajit C. Kunwar<sup>\*,‡</sup>

Contribution from the Organic Chemistry Division III, D-211, Discovery Laboratory, and NMR Group, Indian Institute of Chemical Technology, Hyderabad 500 007, India

Received July 9, 2006; E-mail: esmvee@iict.res.in (G.V.M.S.); kunwar@iict.res.in (A.C.K.)

**Abstract:** New classes of  $\alpha/\gamma$ - and  $\beta/\gamma$ -hybrid peptides have been synthesized with novel 12/10- and 11/13-mixed helical patterns, respectively. The  $\alpha/\gamma$ -peptides were derived from the dipeptide repeats with alternating arrays of L-Ala and  $\gamma$ -Caa<sub>(l)</sub> (C-linked carbo- $\gamma$ -amino acid from D-mannose), which generated a new 12/10-mixed helix, for the first time, without a  $\beta$ -amino acid. The  $\beta/\gamma$ -peptides made from an alternating arrangement of  $\beta$ -Caa<sub>(x)</sub> (C-linked carbo- $\beta$ -amino acid) and  $\gamma$ -Caa<sub>(x)</sub> (C-linked carbo- $\gamma$ -amino acid from D-xylose), on the other hand, resulted in an unprecedented 11/13-helix. The secondary structures in these peptides have been ascertained from detailed NMR studies, and CD spectroscopy and molecular dynamics investigations provided additional support for the structures derived.

### Introduction

Diverse functions carried out by proteins<sup>1</sup> are attributed to their compact three-dimensional structures. Modifications of the peptide backbone with new motifs, while expanding the domain of secondary structural diversity,<sup>2</sup> offer richness in design with desirable properties in the unnatural oligomers. The thrust to mimic essential features of the proteins has led to the discovery of a large variety of secondary structures in the oligomeric scaffolds derived from  $\beta$ -,  $\gamma$ -, and  $\delta$ -amino acids, falling in the domain of "foldamers".<sup>2</sup>  $\beta$ -Peptides, the oligomers of  $\beta$ -amino acids ( $\beta$ -aa), display numerous helices, in addition to turns and  $\beta$ -sheets. 10/12-Helices, with 10- and 12-membered inter-twined H-bonded pseudo-rings with different H-bonded directionalities, are unique to  $\beta$ -peptides. All such mixed helices reported so far contain a motif with a  $\beta$ -aa dipeptide repeat. Seebach et al.,<sup>3</sup> in their design, used alternating  $\beta^2$ - and  $\beta^3$ -amino acids to realize a 12/10-helix, while Kessler et al.<sup>4</sup> generated the 12/10-helix with the dimer repeat of  $\beta$ -aa and  $\beta$ -hGly template. Our group<sup>5</sup> utilized dipeptide repeats derived from epimeric  $\beta$ -Caa's (C-linked carbo- $\beta$ -amino acid) with alternating chirality as well as  $\beta$ -hGly to generate very stable and robust right- and

left-handed 10/12-helices. Further, we have shown in a recent study<sup>6</sup> that  $\alpha/\beta$ -hybrid peptides with heterodimer motif repeats generate unprecedented 9/11-mixed helices, despite having a different backbone geometry. The 9/11-mixed helices are quite robust and were observed in oligomers as short as a tripeptide ( $\alpha$ - $\beta$ - $\alpha$ ).<sup>6</sup> The theoretical studies reported by Wu et al.<sup>7</sup> and Hofmann et al.<sup>8</sup> indicated the mixed helices to be energetically the most favored secondary structures in  $\beta$ -peptides. More recently, via theoretical calculations (ab initio), Hofmann et al.<sup>9</sup> have explored the possibility of forming a variety of helices in  $\alpha/\gamma$ - and  $\beta/\gamma$ -peptides, from which they concluded that, in apolar solvents, the 10/12- or 12/10-mixed helix is the most favored helical structure in  $\alpha/\gamma$ -peptides, while for  $\beta/\gamma$ -peptides, because of the expansion of the H-bonded rings, the lowest energy structure is a 11/13- or 13/11-helix. However, from single-crystal X-ray studies, Balaram et al.<sup>10</sup> have shown that the  $\alpha/\gamma$ -peptides prepared from Aib-Gpn exist as a 12-helix. Inspired by these findings, we report the synthesis of  $\alpha/\gamma$ -peptides 1–5 (Figure

<sup>†</sup> Organic Chemistry Division III.

<sup>‡</sup> NMR Group.

- (1) Hill, D. J.; Mio, M. J.; Prince, R. B.; Hughes, T. S.; Moore, J. S. *Chem. Rev.* **2001**, *101*, 3893–4011.
- (2) (a) Seebach, D.; Beck, A. K.; Bierbaum, D. J. *Chem., Biodiversity* **2004**, *1*, 1111–1239. (b) Cheng, R. P.; Gellman, S. H.; DeGrado, W. F. *Chem. Rev.* **2001**, *101*, 3219–3232.
- (3) (a) Seebach, D.; Gademann, K.; Schreiber, J. V.; Matthews, J. L.; Hintermann, T.; Jaun, B. *Helv. Chim. Acta* **1997**, *80*, 2033–2038. (b) Seebach, D.; Abele, S.; Gademann, K.; Guichard, G.; Hintermann, T.; Juan, B.; Matthews, L. J.; Schreiber, V. J.; Oberer, L.; Hommel, U.; Widmer, H. *Helv. Chim. Acta* **1998**, *81*, 932–982.
- (4) Gruner, S. A. W.; Truffault, V.; Voll, G.; Locardi, E.; Stockle, M.; Kessler, H. *Chem.—Eur. J.* **2002**, *8*, 4366–4376.

- (5) (a) Sharma, G. V. M.; Ravinder Reddy, K.; Radha Krishna, P.; Ravi Sankar, A.; Narsimulu, K.; Kiran Kumar, S.; Jayaprakash, P.; Jagannadh, B.; Kunwar, A. C. *J. Am. Chem. Soc.* **2003**, *125*, 13670–13671. (b) Sharma, G. V. M.; Ravinder Reddy, K.; Radha Krishna, P.; Ravi Sankar, A.; Jayaprakash, P.; Jagannadh, B.; Kunwar, A. C. *Angew. Chem., Int. Ed.* **2004**, *43*, 3961–3965.
- (6) Sharma, G. V. M.; Nagender, P.; Radha Krishna, P.; Jayaprakash, P.; Ramakrishna, K. V. S.; Kunwar, A. C. *Angew. Chem., Int. Ed.* **2005**, *44*, 5878–5882.
- (7) (a) Wu, Y.-D.; Wang, D.-P. *J. Am. Chem. Soc.* **1999**, *121*, 9352–9362. (b) Wu, Y.-D.; Lin, J.-Q.; Zhao, Y.-L. *Helv. Chim. Acta* **2002**, *85*, 3144–3160.
- (8) (a) Mohle, K.; Gunther, R.; Thormann, M.; Sewald, N.; Hofmann, H.-J. *Biopolymers* **1999**, *50*, 167–184. (b) Baldauf, C.; Gunther, R.; Hofmann, H.-J. *Angew. Chem., Int. Ed.* **2004**, *43*, 1594–1597.
- (9) Baldauf, C.; Gunther, R.; Hofmann, H.-J. *J. Org. Chem.* **2006**, *71*, 1200–1208.
- (10) Ananda, K.; Vasudev, P. G.; Sengupta, A.; Raja, K. M. P.; Shamala, N.; Balaram, P. *J. Am. Chem. Soc.* **2005**, *127*, 16668–16674.

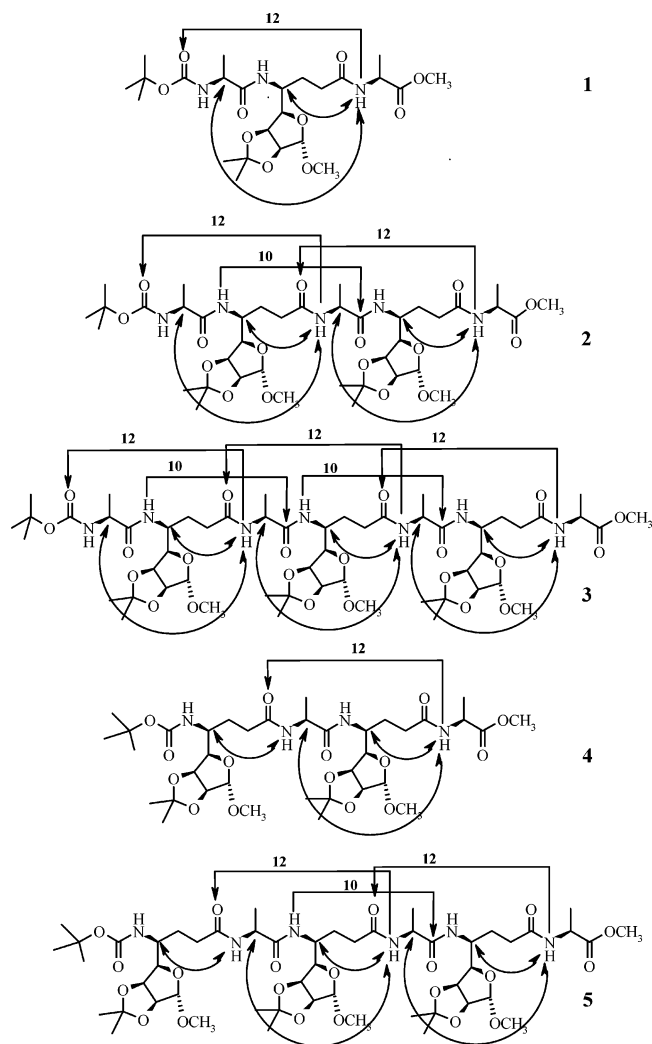


**Figure 1.** Structures of peptides 1–5 (lines with single arrow, H-bonding; lines with double arrows, critical NOEs).

1; from L-Ala and  $\gamma$ -Caa<sub>(l)</sub>, a C-linked carbo- $\gamma$ -amino acid of D-mannose), as the first motif devoid of a  $\beta$ -amino acid for a 12/10-mixed helix, and  $\beta/\gamma$ -peptides 6–8 (Figure 2; from  $\beta$ -Caa<sub>(x)</sub> and  $\gamma$ -Caa<sub>(x)</sub>, C-linked carbo- $\beta$ - and  $\gamma$ -amino acids of D-xylose), with an unprecedented 11/13-mixed helix, and their extensive NMR, CD, and MD studies.

## Results and Discussion

**Synthesis of Peptides 1–8.** The  $\beta$ -Caa and  $\gamma$ -Caa monomers are designed on the basis of the C-(ribofuranoside)-linked glycine moiety present in nikkomycins,<sup>11</sup> which are peptide nucleoside antibiotics. From our earlier studies on the  $\beta$ -Caa-derived peptides<sup>5,6</sup> and the mass spectral fragmentation of the  $\beta$ -Caa-derived dipeptides,<sup>12</sup> it was amply evident that the carbohydrate side chain and the stereochemistry at the amine-bearing stereocenter, indeed, control the conformations in the peptides. The rigidity differences in the “S” and “R” epimeric Caa residues play a crucial role in defining the helical conformations, making them the preferred choice in the present designs. Peptides 1–5 (Scheme 1) were prepared from L-Ala

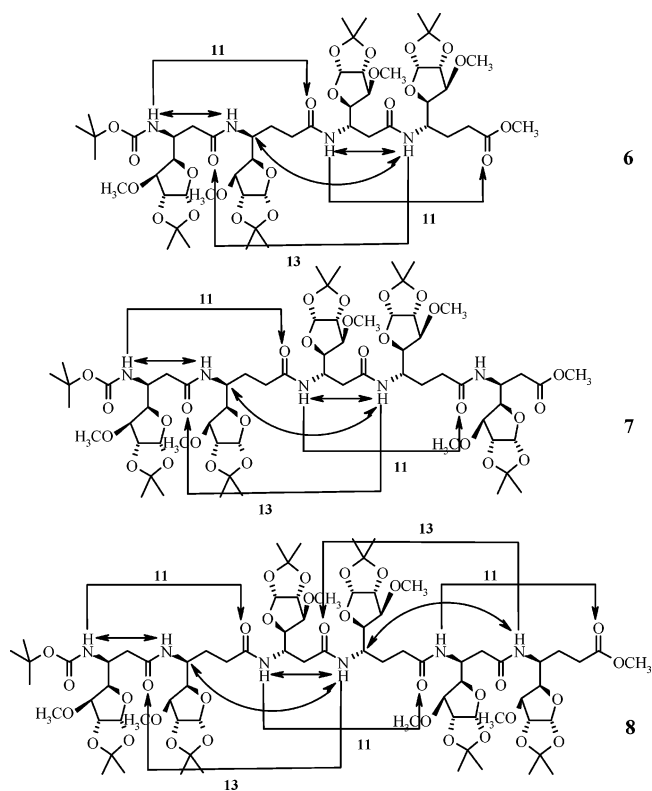


**Figure 2.** Structures of peptides 6–8 (lines with single arrow, H-bonding; lines with double arrows, critical NOEs).

(A) and the new  $\gamma$ -Caa<sub>(l)</sub> (9),<sup>13</sup> while 6–8 (Scheme 2) were synthesized from  $\beta$ -Caa<sub>(x)</sub> (22)<sup>14</sup> and  $\gamma$ -Caa<sub>(x)</sub> (23)<sup>15</sup> by standard peptide coupling methods (EDCI/HOBt and DIPEA) in solution phase.

Accordingly,  $\gamma$ -Caa<sub>(l)</sub>-OMe (9, Scheme 1), on exposure to CF<sub>3</sub>COOH in CH<sub>2</sub>Cl<sub>2</sub>, was converted into the salt 11, which on condensation with acid 12 in the presence of EDCI/HOBt and DIPEA in CH<sub>2</sub>Cl<sub>2</sub> afforded the dipeptide 13. Ester 13, on base-mediated hydrolysis (4 N NaOH), was converted into the corresponding acid 14, which on further peptide coupling furnished the tripeptide 1. Acid 10, obtained by base hydrolysis from 9, was coupled with 15 to give the dipeptide 17, which on exposure to CF<sub>3</sub>COOH in CH<sub>2</sub>Cl<sub>2</sub> afforded 19. The salt 19 was then coupled with acid 16 (prepared by base hydrolysis of ester 1) in the presence of EDCI/HOBt and DIPEA in CH<sub>2</sub>Cl<sub>2</sub> to afford the pentapeptide 2, which on hydrolysis with base (4 N NaOH) and peptide coupling of acid 20 with salt 19 furnished the heptapeptide 3. Further coupling of acid 18 with salt 19 afforded the tetrapeptide 4. Similarly, base-mediated hydrolysis of 4 gave the acid 21, which on further coupling with amine 19 furnished the hexapeptide 5.

The  $\beta/\gamma$ -peptides 6–8 (Figure 2), having a N-terminus  $\beta$ -Caa<sub>(x)</sub>, were prepared by adopting the above procedure. Thus, the ester group in 22 (Scheme 2) was saponified with 4 N NaOH to give acid 25, which on coupling with 26 (prepared by the exposure of 23 to CF<sub>3</sub>COOH) gave dipeptide 27. Base hydrolysis of ester 27 and coupling of the resulting acid 29 with the

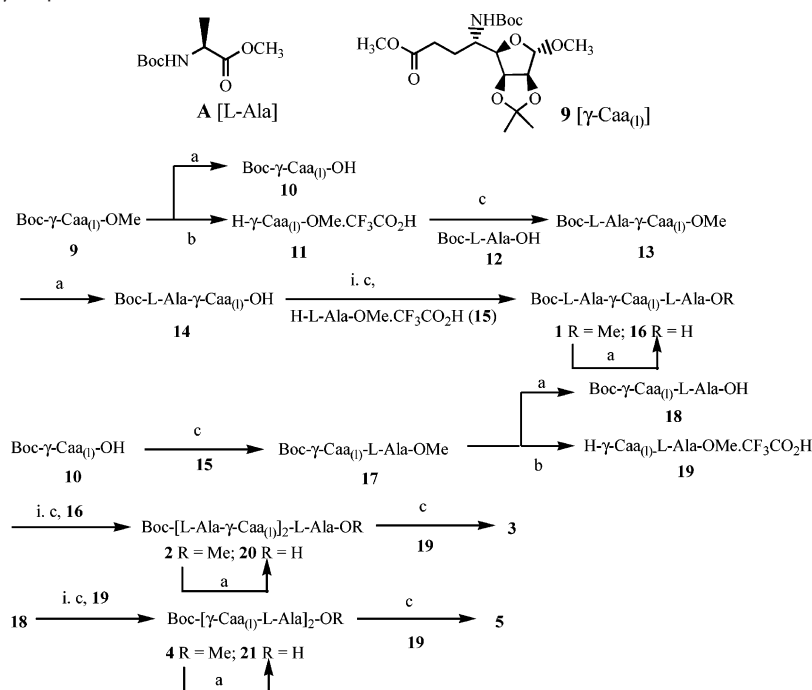
(13) See Supporting Information.

(14) Sharma, G. V. M.; Goverdhan Reddy, V.; Subahsh Chander, A.; Ravinder Reddy, K. *Tetrahedron: Asymmetry* **2002**, *13*, 21–24.

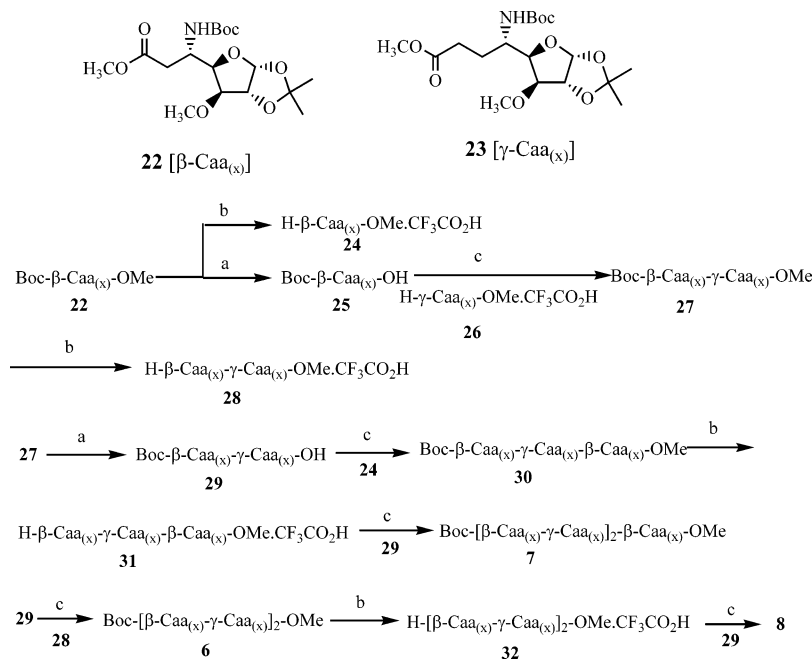
(15) Sharma, G. V. M.; Jayaprakash, P.; Narsimulu, K.; Ravi Sankar, A.; Ravinder Reddy, K.; Radha Krishna, P.; Kunwar, A. C. *Angew. Chem., Int. Ed.* **2006**, *45*, 2944–2947.

(11) Barrett, A. G.; Lebold, S. J. *Org. Chem.* **1991**, *56*, 4875–4884.

(12) Srikanth, R.; Nagi Reddy, P.; Narsimha, R.; Srinivas, R.; Sharma, G. V. M.; Ravinder Reddy, K.; Radha Krishna, P. *J. Mass Spectrom.* **2004**, *39*, 1068–1074.

**Scheme 1.** Synthesis of  $\alpha/\gamma$ -Peptides 1–5<sup>a</sup>

<sup>a</sup> Reagents and conditions: (a) aqueous 4 N NaOH, MeOH, 0 °C to room temperature, 2 h; (b) CF<sub>3</sub>COOH, dry CH<sub>2</sub>Cl<sub>2</sub>, 2 h; (c) HOBt (1.2 equiv), EDCI (1.2 equiv), DIPEA (2 equiv), dry CH<sub>2</sub>Cl<sub>2</sub>, 0 °C to room temperature, 4 h.

**Scheme 2.** Synthesis of  $\beta/\gamma$ -Peptides 6–8<sup>a</sup>

<sup>a</sup> Reagents and conditions: (a) aqueous 4 N NaOH, MeOH, 0 °C to room temperature, 2 h; (b) CF<sub>3</sub>COOH, dry CH<sub>2</sub>Cl<sub>2</sub>, 2 h; (c) HOBt (1.2 equiv), EDCI (1.2 equiv), DIPEA (2 equiv), dry CH<sub>2</sub>Cl<sub>2</sub>, 0 °C to room temperature, 4 h.

salt **24** (obtained from **22** by exposure to CF<sub>3</sub>COOH) gave tripeptide **30**. Acid-mediated Boc-group deprotection in **30** gave the salt **31**, which on coupling with acid **29** afforded pentapeptide **7**.

Likewise, the peptides **6** and **8** (Scheme 2) were prepared using the dipeptide acid and amine salts **29** and **28**, respectively. Accordingly, **29**, on coupling with **28**, afforded the tetrapeptide **6**, which on exposure to CF<sub>3</sub>COOH gave the amine salt **32**. Further coupling of **32** with acid **29** afforded hexapeptide **8**.

## Conformational Analysis

Recent theoretical studies by Hofmann et al.<sup>9</sup> on  $\alpha/\gamma$ - and  $\beta/\gamma$ -hybrid peptides indicate that, while a variety of helices in  $\alpha/\gamma$ -peptides resemble structures structurally those derived from  $\beta$ -dipeptide repeats,  $\beta/\gamma$ -hybrid peptides demonstrate structural similarities with those obtainable with tripeptide repeats derived from  $\alpha$ -amino acids. The classification described by Hofmann's group shows that the mixed helices obtained from these hybrid

peptides differ in subtle ways, depending upon how the H-bonds in the forward and the backward directions are formed. For  $\alpha/\gamma$ -peptides, when the amide proton of the  $\alpha$ -residue is involved in a 10-membered H-bond and the amide proton of the  $\gamma$ -amino acid participates in 12-membered H-bond, the helix is referred to as a 10/12-helix. On the other hand, when the 10- and 12-membered rings involve the amide protons of the  $\gamma$ - and  $\alpha$ -residues respectively, the secondary structure is denoted as a 12/10-helix. Likewise, in  $\beta/\gamma$ -peptides, the mixed helix is termed as an 11/13-helix when the amide protons of the  $\beta$ - and  $\gamma$ -residues take part in 11- and 13-membered H-bonds, respectively, whereas, if the H-bonding pattern involves the participation of the amide proton of the  $\gamma$ -residue in the 11-membered ring and that of the  $\beta$ -residue in the 13-membered ring, the helix is referred to as a 13/11-helix.

**$\alpha/\gamma$ -Peptides.** In the  $^1\text{H}$  NMR spectrum of the trimer **1** (Figure 1) in  $\text{CDCl}_3$ ,<sup>13</sup> the Ala(3) amide resonance at  $\delta\text{NH} = 7.36$  ppm indicated its participation in H-bonding, which was further confirmed by solvent titration studies<sup>16</sup> ( $\Delta\delta\text{NH} = 0.55$  ppm), as shown in Figure 3. For  $\gamma$ -Caa(2),  $^3J_{\text{NH}-\text{C}\gamma\text{H}} = 8.8$  Hz suggests  $\text{C}(\text{O})-\text{N}-\text{C}\gamma-\text{C}\beta$  ( $\phi_\gamma$ )  $\approx 120^\circ$ , while the  $^3J_{\text{C}\beta\text{H}-\text{C}\gamma\text{H}}$  values of 8.8 and 5.1 Hz indicate the preponderance of a structure with  $\text{N}-\text{C}\gamma-\text{C}\beta-\text{C}\alpha$  ( $\theta_{1\gamma}$ )  $\approx -60^\circ$  or  $180^\circ$ . Though the presence of strong  $\text{C}\alpha\text{H}(1)/\text{NH}(2)$  allowed us to fix  $\text{N}-\text{C}\alpha-\text{C}(\text{O})-\text{N}$  ( $\psi_\alpha$ )  $\approx 120^\circ$  for the Ala(1) residue, additional information, in the form of the characteristic nuclear Overhauser effects (NOEs),  $\text{C}\alpha\text{H}(1)/\text{NH}(3)$  and  $\text{C}\gamma\text{H}(2)/\text{NH}(3)$ , was not sufficient to fully characterize the structure. Even though many of these features are the critical signatures of 12/10- and 11/9-mixed helices, to ascertain more definitive information on the secondary structure of **1**, the larger peptides **2** and **3** were investigated.

In the pentapeptide **2** (Figure 1), NH(2), NH(3), and NH(5) resonances appeared at low field ( $\delta\text{NH} > 7$  ppm), while small values of  $\Delta\delta\text{NH} < 0.24$  ppm in the solvent titration studies (Figure 3) confirm their involvement in H-bonding.  $^3J_{\text{NH}-\text{C}\alpha\text{H}} = 6.0$  Hz for Ala(3) suggests a preponderance of a single structure with constrained  $\text{C}(\text{O})-\text{N}-\text{C}-\text{C}(\text{O})$  ( $\phi_\alpha$ ), whereas the corresponding values for Ala(1) and Ala(5) of about 7 Hz may either arise from a single predominant conformation or be due to fraying in the termini, resulting in the averaging due to structures with several values of  $\phi_\alpha$ . Strong  $\text{C}\alpha\text{H}(1)/\text{NH}(2)$  and  $\text{C}\alpha\text{H}(3)/\text{NH}(4)$  NOEs further suggest  $\psi_\alpha \approx 120^\circ$  for the Ala(1) and Ala(3) residues. For  $\gamma$ -Caa(2) and  $\gamma$ -Caa(4) residues,  $^3J_{\text{NH}-\text{C}\gamma\text{H}}$  value of 9.0 and 9.5 Hz, respectively, suggest that  $\phi_\gamma \approx 120^\circ$ , and the  $^3J_{\text{C}\beta\text{H}-\text{C}\gamma\text{H}}$  values of 9.4 and 5.5 Hz for  $\gamma$ -Caa(4) indicate a propensity of structures with  $\theta_{1\gamma} \approx -60^\circ$  or  $180^\circ$ . Due to spectral overlap, it was not possible to get individual chemical shifts and most of the coupling constants involving  $\text{C}\alpha\text{H}$  and  $\text{C}\beta\text{H}$  protons of  $\gamma$ -Caa. However, assuming that only staggered conformations are preferred about  $\text{C}\alpha-\text{C}\beta$ , NOE correlations  $\text{C}\gamma\text{H}(2)/\text{NH}(3)$ ,  $\text{NH}(2)/\text{NH}(3)$ ,  $\text{C}\gamma\text{H}(4)/\text{NH}(5)$ , and  $\text{NH}(4)/\text{NH}(5)$  were found to support conformations with only  $\theta_{1\gamma} \approx -60^\circ$ ,  $\text{C}\gamma-\text{C}\beta-\text{C}\alpha-\text{C}(\text{O})$  ( $\theta_{2\gamma}$ )  $\approx 60^\circ$ , and  $\text{C}\beta-\text{C}\alpha-\text{C}(\text{O})-\text{N}$  ( $\psi_\gamma$ )  $\approx -120^\circ$ . Such structures are also consistent with strong  $\text{C}3\text{H}/\text{C}\beta\text{H}$ ,  $\text{C}4\text{H}/\text{C}\beta\text{H}$ , and  $\text{NH}/\text{C}4\text{H}$  intra-residue NOEs involving sugar ring protons. The distinctive NOEs (Figure 4),

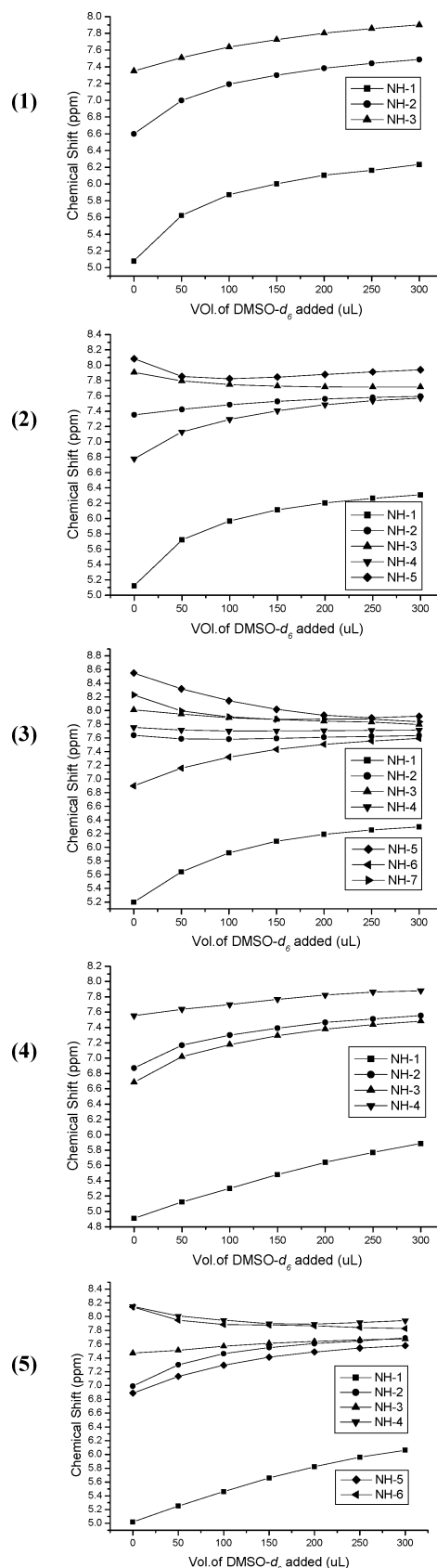


**Figure 3.** Solvent titration studies of peptides **1–5**.

$\text{C}\alpha\text{H}(1)/\text{NH}(3)$ ,  $\text{NH}(2)/\text{NH}(3)$ ,  $\text{C}\alpha\text{H}(3)/\text{NH}(5)$ , and  $\text{NH}(4)/\text{NH}(5)$ , along with the dihedral angles and H-bonding information deduced above, provide compelling evidence for the presence of a right-handed 12/10-helix involving  $\text{NH}(3)-\text{Boc}$

(16) Solvent titration studies were carried out by sequentially adding up to 50% of  $\text{DMSO}-d_6$  to 600  $\mu\text{L}$  of  $\text{CDCl}_3$  solutions of the peptides. Small changes in amide proton chemical shift ( $\Delta\delta\text{NH}$ ) have been used as an indication for H-bonding.

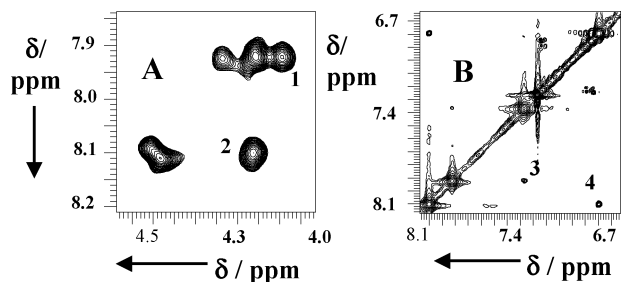


**Figure 4.** ROESY spectrum of **2**. (A) NOEs C $\alpha$ H(1)/NH(3) and C $\alpha$ H(3)/NH(5) are marked as 1 and 2, respectively. (B) NOEs NH(2)/NH(3) and NH(4)/NH(5) are marked as 3 and 4, respectively.

CO, NH(2)–CO(3), and NH(5)–CO(2) H-bonds corresponding to a 12/10/12-helical configuration. For NH(4),  $\delta$ NH = 6.80 ppm and  $\Delta\delta$ NH = 0.79 ppm in the solvent titration studies<sup>16</sup> reflect fraying of the peptide at the C-terminus, probably with a small population of molecules having the expected H-bond between NH(4) and CO(5). Nondescript values of  $^3J_{\text{NH}-\text{C}\alpha\text{H}}$  for the terminal Ala residues also support this observation. Strong evidence for the propagation of the 12/10-helix was also observed in **3**, and unequivocal evidence for a 12/10/12/10 H-bonding configuration was derived from the data.<sup>13</sup>

The study was further extended to the tetrapeptide **4** and hexapeptide **5**, with  $\gamma$ -Caa at the N-terminus. For both **4** and **5**, though several amide protons show their involvement in H-bonding as deduced from  $\delta$ NH and the solvent titration studies (Figure 3), the first, second, and next-to-last amide protons do not seem to have significant populations of such H-bonds. The value  $^3J_{\text{NH}-\text{C}\gamma\text{H}} > 9.0$  Hz is consistent with  $\phi_\gamma \approx 120^\circ$ . For **4**, with only one distinct H-bonded amide proton, the evidence for nucleation of a helical structure is provided by C $\alpha$ H(2)/NH(4), NH(3)/NH(4), C $\gamma$ H(1)/NH(2), and C $\gamma$ H(3)/NH(4) NOE correlations. For **5**,  $^3J_{\text{NH}-\text{C}\alpha\text{H}} \approx 6$  Hz for Ala(2) and Ala(4) (at 250.5 K), which supports the presence of a single dominant conformation about N–C $\alpha$ . Strong C $\alpha$ H(2)/NH(3) and C $\alpha$ H(4)/NH(5) NOEs further suggest  $\psi_\alpha \approx 120^\circ$  for these residues. The NOE correlations C $\alpha$ H(2)/NH(4), C $\alpha$ H(4)/NH(6), NH(3)/NH(4), NH(5)/NH(6), C $\gamma$ H(3)/NH(4), and C $\gamma$ H(5)/NH(6), in addition to the information on dihedral angles and H-bonds, support a 12/10-helix. Further,  $\delta$ NH = 6.89 ppm and  $\Delta\delta$ NH = 0.70 ppm for NH(5) imply the presence of a sizable population of structures with involvement of the amide proton in a 10-membered H-bond, indicating a putative 12/10/12/10 H-bonding pattern in **5**.

For  $\gamma$ -Caa, the value  $^3J_{\text{C}\gamma\text{H}-\text{C}4\text{H}} > 9$  Hz implies  $\chi_1(\gamma)(\text{C}\gamma\text{H}-\text{C}\gamma-\text{C}(4)-\text{C}(4)\text{H}) \approx 180^\circ$  for all the peptides, which is similar to earlier observations.<sup>5,6</sup> The sugar ring couplings of  $^3J_{\text{C}1\text{H}-\text{C}2\text{H}} \approx 0$  Hz,  $^3J_{\text{C}2\text{H}-\text{C}3\text{H}} \approx 5.9$  Hz, and  $^3J_{\text{C}3\text{H}-\text{C}4\text{H}} \approx 3.6$  Hz are in conformity with the <sup>2</sup>T<sub>3</sub> sugar pucker for the furanose ring.

Further, the NMR studies<sup>13</sup> on peptides **2** and **5** were carried out in methanol to understand the stability of the helices in a polar solvent. The NH–D exchange studies carried out in CD<sub>3</sub>OD show that all the amide protons exchange fully within 2 h, thereby ruling out their involvement in intramolecular H-bonding. Similarly, changes in amide proton chemical shift with respect to temperature ( $\Delta\delta/\Delta T$ ), having a magnitude greater than 9 ppb/K, for all the amides in these peptides support the above observation. It is, however, worth mentioning that studies in CD<sub>3</sub>OH found some of the distinct signatures of a 12/10-helix, like NOEs C $\alpha$ H(1)/NH(3) and C $\alpha$ H(3)/NH(5) in

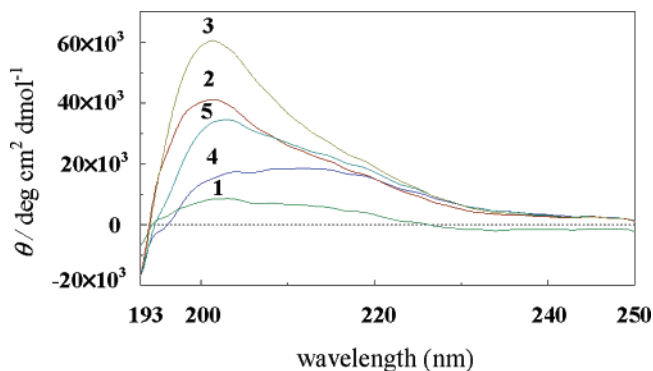


**Figure 5.** CD spectra of peptides **1–5**.

peptide **2** and C $\alpha$ H(2)/NH(4) and C $\alpha$ H(4)/NH(6) in **5**, with very low intensities. This implies that a 12/10-helix exists in methanol with very low propensity. These observations are consistent with the suggestion of destabilization of mixed helices in polar solvents.<sup>9</sup>

The CD spectra<sup>13</sup> of **1–5** (Figure 5) in MeOH (0.2 mM), with a prominent maximum at 203 nm and an extended tail with a broad peak centered around 220 nm, support the presence of a secondary structure. These signatures resemble those of the right-handed 12/10-mixed helix.<sup>3,5</sup>

In the restrained molecular dynamics (MD) studies (Figure 6), constraints were derived from the volume integrals obtained from the ROESY spectra using a two-spin approximation. Panels A and B of Figure 6 show the 20 lowest energy superimposed structures of **3** and **5**, respectively. The root-mean-square deviations (rmsd's) of the backbone and the heavy atoms for **3** are 0.66 and 0.89 Å (Figure 6A), respectively, while the corresponding values for **5** are 0.45 and 0.58 Å (Figure 6B). The average values of the dihedral angles (excluding the residues in the C- and N-termini) in **3** are  $\phi_\alpha = -69 \pm 3^\circ$ ,  $\psi_\alpha = 134 \pm 5^\circ$ ,  $\phi_\gamma = 139 \pm 3^\circ$ ,  $\theta_{1\gamma} = -52 \pm 5^\circ$ ,  $\theta_{2\gamma} = 101 \pm 3^\circ$ , and  $\psi_\gamma = -104 \pm 3^\circ$ , whereas the corresponding values for **5** are  $-67 \pm 1^\circ$ ,  $140 \pm 4^\circ$ ,  $139 \pm 3^\circ$ ,  $-55 \pm 2^\circ$ ,  $99 \pm 1^\circ$ , and  $-104 \pm 1^\circ$ . The observed dihedral angles agree very well with the corresponding values of  $62^\circ$ ,  $-151^\circ$ ,  $-129^\circ$ ,  $51^\circ$ ,  $-96^\circ$ , and  $120^\circ$  for the second most favored 12/10-helix (left-handed) in Hoffman's<sup>9</sup> recent study; however, they differ in sign, reflecting the difference in the handedness of the helical structures.

A comparative study on the 12/10-helices derived from the  $\alpha/\gamma$ -hybrid peptides in the present work and those observed in  $\beta$ -peptides<sup>7b</sup> has been made and is depicted in Figure 7. The 12/10-helix in the  $\alpha/\gamma$ -peptides has a pitch of  $\sim 6.2$  Å, with  $\sim 2.8$  residues/turn and a  $\sim 2.2$  Å rise/residue, which differs slightly from the pitch of  $\sim 5.7$  Å, 2.7 residues/turn, and 2.1 Å rise/residue for the 12/10-helix in  $\beta$ -peptides.

**$\beta/\gamma$ -Peptides.** We have investigated three oligomers, **6–8** (Figure 2), from this class of molecules.<sup>17</sup> In the  $\beta/\gamma$ -tetrapeptide **6**, two amide resonances appear at  $\delta$ NH  $> 7$  ppm. Solvent titration studies<sup>16</sup> (Figure 8) show that, excluding NH(2), the other amide resonances shift by  $< 0.52$  ppm, confirming their participation in hydrogen bonding. For both  $\beta$ -residues,  $^3J_{\text{NH}-\text{C}\beta\text{H}} > 9.3$  Hz, suggesting an antiperiplanar (*ap*) arrangement for these protons, which corresponds to CO–N–C $\beta$ –C $\alpha$  ( $\phi_\beta$ )  $\approx 120^\circ$ . Among the  $\beta$ -residues, the information on N–C $\beta$ –C $\alpha$ –

(17) Of the two isomers observed in peptides **6–8**, the results pertaining to the major isomer are presented (minor isomer population was less than 10%).

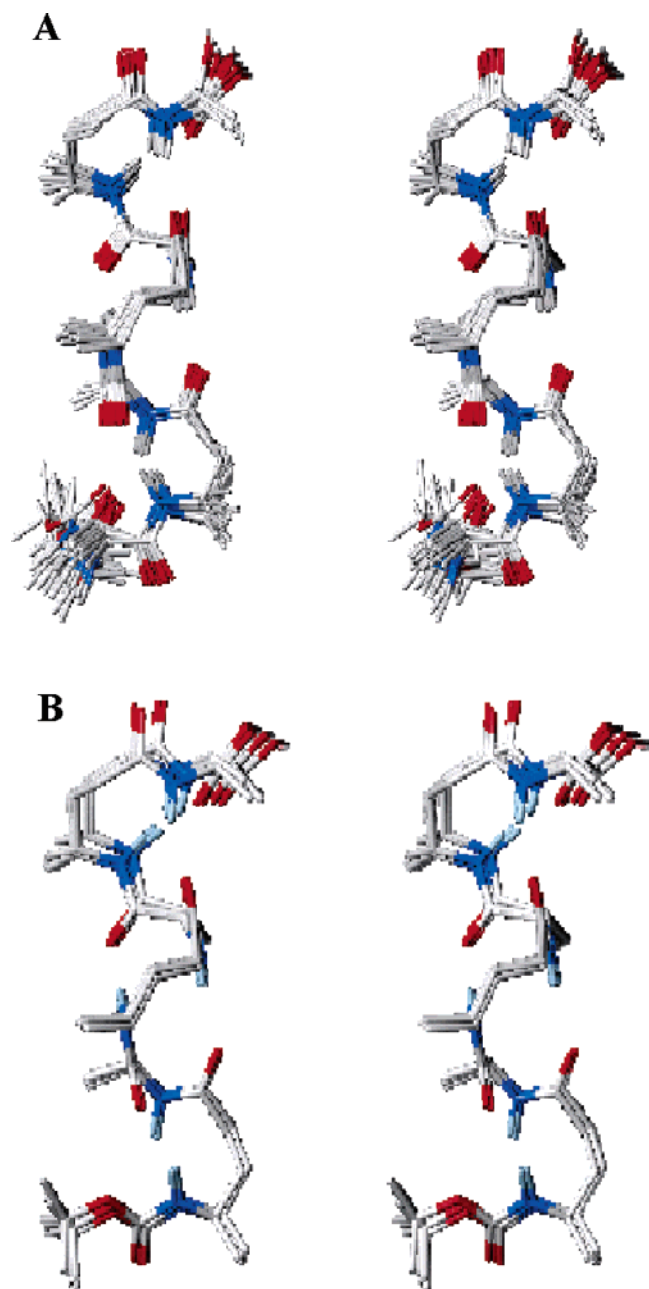


**Figure 6.** Stereoviews of (A) peptide 3 and (B) peptide 5. Sugars are replaced with methyl groups after calculations.

CO ( $\theta_\beta$ ) for the first residue could be easily derived from small values of both  $^3J_{\text{C}\alpha\text{H}-\text{C}\beta\text{H}}$  ( $\sim 5$  Hz), which is consistent with  $\theta_\beta \approx 60^\circ$ . This information, along with the C $\alpha$ H(1)/NH(1) and C $\alpha$ H(1)/NH(2) NOEs, permits us to assign C $\alpha$ H(*pro-R*)(1) as having stronger NOEs with NH(1) and NH(2) compared to C $\alpha$ H(*pro-S*)(1). Further, the observation of NH(1)/NH(2) and C4H(1)/NH(2) NOE correlations suggests a C $\beta$ -C $\alpha$ -CO-N ( $\psi_\beta$ ) value in the vicinity of  $0^\circ$ . Similar observations of NOEs C $\alpha$ H(3)/NH(3), C $\alpha$ H(3)/NH(4), NH(3)/NH(4), and C4H(3)/NH(4), involving the third and the fourth residues, permit stereospecific assignment of protons at C $\alpha$ (3) and are consistent with  $\theta_\beta \approx 60^\circ$ ,  $\psi_\beta \approx 0^\circ$ .

For the  $\gamma$ -residues,  $^3J_{\text{NH}-\text{C}\gamma\text{H}} = 8.2$  and  $9.6$  Hz for the second and fourth residues, respectively, suggesting a preponderance of *ap* arrangement of NH and C $\gamma$ H, corresponding to a value of around  $120^\circ$  for  $\phi_\gamma$ . Due to spectral overlap, the detailed

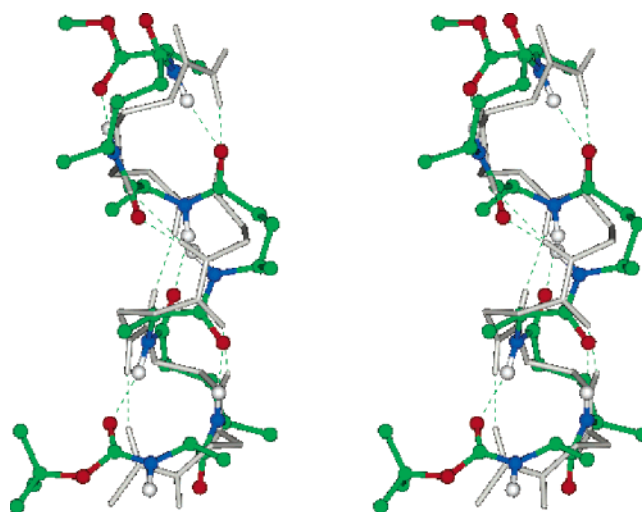


**Figure 7.** Stereoview of the overlay of the 12/10-mixed helices of peptide 3 ( $\alpha/\gamma$ -peptide is indicated with ball-and-stick model) and  $\beta$ -peptide (hexapeptide of  $\beta$ -hGly residues with N- and C-termini having acetyl and amide groups, respectively).<sup>7b</sup> In 3, sugars are replaced with methyl groups after calculations.

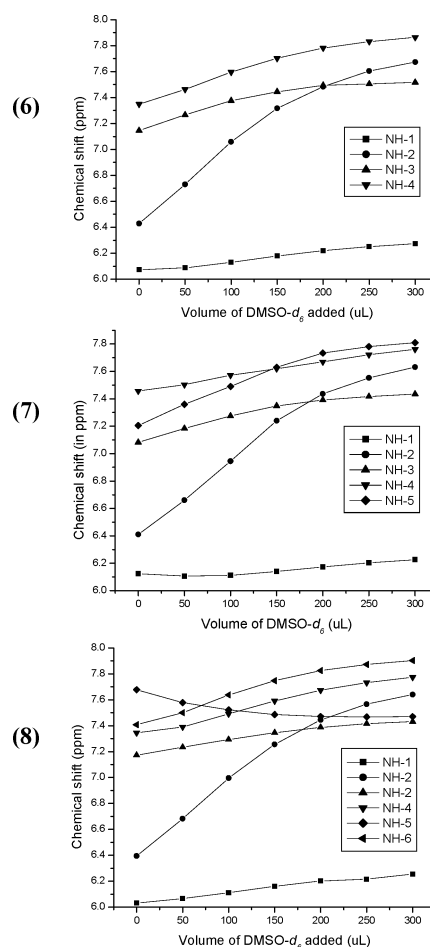


**Figure 8.** Solvent titration studies of peptides 6–8.

coupling pattern could be deciphered only for a few C $\alpha$ H and C $\beta$ H protons. The stereospecific assignments for C $\beta$ H protons could be made on the basis of the couplings and NOEs. The  $^3J_{\text{C}\beta\text{H}-\text{C}\gamma\text{H}}$  values,  $< 5.0$  and  $> 9.0$  Hz, imply that  $\theta_{1\gamma} \approx -60^\circ$  or  $180^\circ$ , such that one of the C $\beta$ H protons is *ap* whereas the other is synclinal with respect to the C $\gamma$ H. The strong intra-residue NOEs between one of the C $\beta$ H (*ap* with respect to C $\gamma$ H)

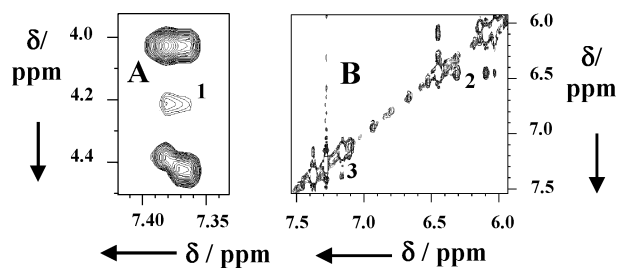


**Figure 9.** ROESY spectrum of **6**. (A) NOE C $\gamma$ H(2)/NH(4) is marked as 1. (B) NOEs NH(1)/NH(2) and NH(3)/NH(4) are marked as 2 and 3, respectively.

and the NH and C4H of the sugar ring helped us to assign them as C $\beta$ H(*pro-R*), confirming  $\theta_{1\gamma} \approx -60^\circ$ . Stereospecific assignments for C $\alpha$ H protons in the  $\gamma$ -residues were possible only for C $\alpha$ H(2) protons. One of the C $\alpha$ H protons resonated at  $\delta$  2.30, with  $^3J_{\text{C}\alpha\text{H}-\text{C}\beta\text{H}} = 4.9$  and 9.1 Hz, whereas the other one appeared at  $\delta$  2.25, with  $^3J_{\text{C}\alpha\text{H}-\text{C}\beta\text{H}} = 5.2$  and 6.9 Hz. These values arise from structures with predominately  $\theta_{2\gamma} \approx 60^\circ$  and permit assigning C $\alpha$ H(*pro-R*) at  $\delta$  2.30. Additionally, observation of NOEs between NH(3) and both the C $\alpha$ H(2) and C $\gamma$ H(2) protons is consistent only with  $\theta_{2\gamma} \approx 60^\circ$  and  $\psi_\gamma \approx -120^\circ$ .

A characteristic medium-range NOE (Figure 9), C $\gamma$ H(2)/NH(4), similar to that observed in 9/11- and 10/12-helices, strongly supports mixed helical structure with a 13-membered NH(4)–CO(1) H-bond. We also observed the NH(1)/NH(2) and NH(3)/NH(4) NOEs, similar to those for the 10/12-helix discussed above, suggesting the presence of 11-membered NH(1)–CO(2) and NH(3)–CO(4) H-bonds. These considerations provide compelling evidence for a hitherto not reported 11/13-helix, with an 11/13/11 H-bonded arrangement in **6**.

For the pentapeptide **7**, NMR data support a structure very similar to that for **6**. The low-field chemical shifts of the amide protons and solvent titration studies show that NH(1), NH(3), and NH(4) are H-bonded. Additionally, from large  $^3J_{\text{NH}-\text{C}\beta\text{H}}$  and  $^3J_{\text{NH}-\text{C}\gamma\text{H}}$  values,  $\phi_\beta$  and  $\phi_\gamma$  are inferred to be around  $120^\circ$ . Comprehensive information on  $\theta_\beta$ ,  $\theta_{1\gamma}$ , and  $\theta_{2\gamma}$ , similar to that for **6**, from the couplings and the NOEs has been obtained and is discussed in the Supporting Information.<sup>13</sup> The data provide adequate support for a 11/13-mixed helix with an 11/13/11 H-bonding pattern in **7**.

In hexapeptide **8**, extensive exchange peaks in the TOCSY/ROESY spectra preclude a detailed structural analysis. However, in the major isomer, all amides, excluding NH(2), participate in H-bonding (Figure 8). Additionally,  $^3J_{\text{NH}-\text{C}\beta\text{H}}$  in  $\beta$ -Caa and  $^3J_{\text{NH}-\text{C}\gamma\text{H}}$  in  $\gamma$ -Caa, with large values, support a structure similar to those of **6** and **7**. Details on other couplings were rather difficult to obtain due to the broadening and dominance of the exchange between the two rotamers. However, some of the NOE details, like C $\gamma$ H(2)/NH(4), C $\gamma$ H(4)/NH(6), NH(1)/NH(2), and NH(3)/NH(4), provide additional evidence for the underlying structure. Observation of a CD spectrum very similar to that of **6** (Figure 10) further confirms the presence of an extended 11/13-helical structure for **8**.

Sugar couplings,  $^3J_{\text{C1H}-\text{C2H}} \approx 3.8$  Hz,  $^3J_{\text{C2H}-\text{C3H}} \approx 0$  Hz, and  $^3J_{\text{C3H}-\text{C4H}} \approx 3.2$  Hz, for both  $\beta$ -Caa and  $\gamma$ -Caa correspond to the sugar pucker  $^3T_2$ , which is similar to the earlier observations.<sup>5,6</sup> For  $\beta$ -residues,  $^3J_{\text{C}\beta\text{H}-\text{C4H}} \approx 9$  Hz, corresponding to  $\chi_1(\beta)(\text{C}\beta\text{H}-\text{C}\beta-\text{C4}-\text{C4H}) \approx 180^\circ$  in all the oligomers. For the second residue,  $^3J_{\text{C}\gamma\text{H}-\text{C4H}} \approx 2.8$  Hz suggests  $\chi_1(\gamma)(\text{C}\beta\text{H}-\text{C}\beta-\text{C4}-\text{C4H}) \approx |60^\circ|$ .

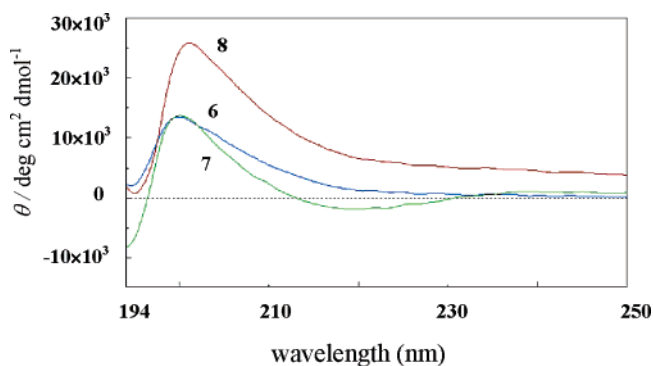


**Figure 10.** CD spectra of peptides **6–8**.

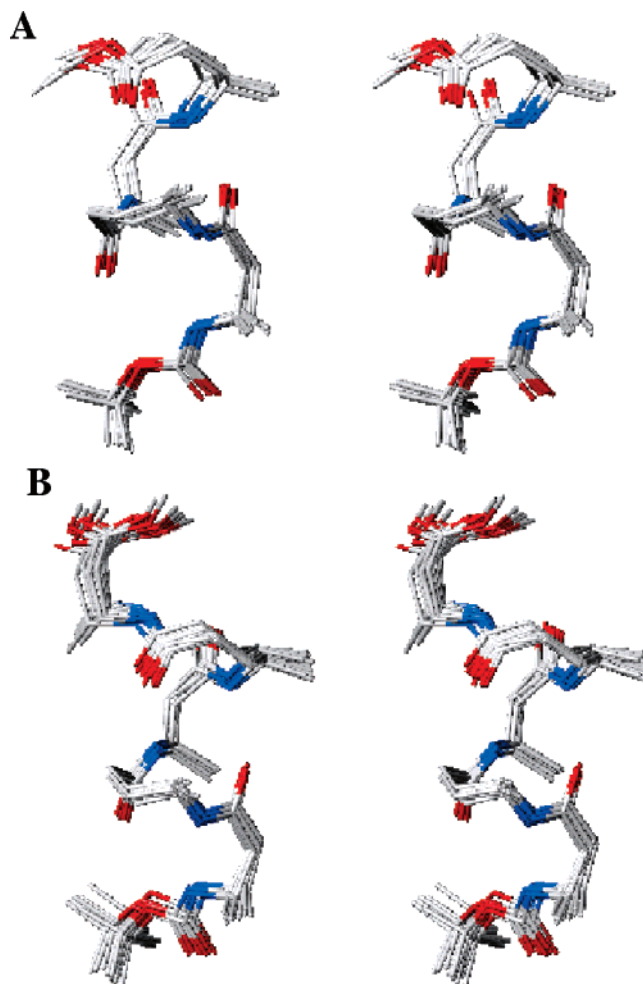


**Figure 11.** Stereoviews of (A) peptide **6** and (B) peptide **7**. Sugars are replaced with methyl groups after calculations.

Further, considerable destabilization of the helical structure is indicated by the weak signatures of the helices from the NOE data of **7** in CD<sub>3</sub>OH.<sup>13</sup> These observations are consistent with the conclusions of Hofmann et al.<sup>9</sup> on the stability of the mixed helices in polar solvents.

For **6–8**, the CD spectra are shown in the Figure 10. The basic features are very similar to those observed for the  $\alpha/\gamma$ -peptides **1–5**.

Figure 11 shows the 20 lowest energy superimposed structures of **6** and **7** from the MD studies. The rmsd's of the backbone and the heavy atoms for **6** (Figure 11A) are 0.41 and 0.61 Å, whereas for **7** (Figure 11B) the corresponding values are 0.49

and 0.92 Å. The average values of the dihedral angles (excluding residues at the C- and N-termini) in **6** are  $\phi_\beta = 142 \pm 4^\circ$ ,  $\theta_\beta = 66 \pm 2^\circ$ ,  $\psi_\beta = -10 \pm 4^\circ$ ,  $\phi_\gamma = 121 \pm 2^\circ$ ,  $\theta_{1\gamma} = -81 \pm 2^\circ$ ,  $\theta_{2\gamma} = 58 \pm 2^\circ$ , and  $\psi_\gamma = -101 \pm 3^\circ$ , while those for **7** are  $\phi_\beta = 145 \pm 5^\circ$ ,  $\theta_\beta = 68 \pm 3^\circ$ ,  $\psi_\beta = -8 \pm 6^\circ$ ,  $\phi_\gamma = 123 \pm 3^\circ$ ,  $\theta_{1\gamma} = -84 \pm 3^\circ$ ,  $\theta_{2\gamma} = 63 \pm 4^\circ$ , and  $\psi_\gamma = -106 \pm 4^\circ$ , respectively. These values agree with those for the higher energy 11/13<sup>III</sup>-helix reported by Hofmann et al.<sup>9</sup> The helical parameters for the 11/13-helix are  $\sim 2.7$  residues/turn,  $\sim 2.2$  Å rise/residue, and pitch  $\approx 5.9$  Å.

A comparison of the positioning and directionalities of the carbohydrate side chains indicates that, in the  $\alpha/\gamma$ -hybrid peptides, the methyl group of L-Ala is placed in the equatorial position, whereas the backbone C $\gamma$ -C4 (of the sugar ring) bond is placed along the helix axis, while, for the  $\beta/\gamma$ -peptides, the side chains at the  $\beta$ -residues are appended axially, whereas those in the  $\gamma$ -residues take an equatorial orientation.

## Conclusions

The present study reports the synthesis and conformational analysis of hybrid  $\alpha/\gamma$ - and  $\beta/\gamma$ -peptides. It presents (a) a new 12/10-mixed helix motif in  $\alpha/\gamma$ -peptide without a  $\beta$ -amino acid and (b) a hitherto unknown 11/13-mixed helix in the  $\beta/\gamma$ -peptides. Further, our new design gives the first experimental proof to Hofmann's<sup>9</sup> recent predictions of the secondary structures in  $\alpha/\gamma$ - and  $\beta/\gamma$ -peptides. Since the mixed peptide domain has been dominated by  $\beta$ -peptides, whereas  $\gamma$ -peptides do not display stable mixed helices, the availability of such novel motifs, which combine higher homologues of  $\alpha$ -amino acids, not only considerably enhances the repertoire of designs and secondary structures in the foldamer domain but also may allow for generation of new materials.

## Experimental Section

NMR spectra (1D and 2D experiments) for peptides **1–8** were obtained at 500 and 600 MHz (<sup>1</sup>H) and at 75 and 150 MHz (<sup>13</sup>C). Chemical shifts are reported in  $\delta$  scale with respect to internal tetramethylsilane reference. IR spectra were recorded with an FT-IR spectrometer between 400 and 4000 cm<sup>-1</sup> in KBr pellets. Melting points were determined in open capillaries and were not corrected.

The CD spectra were obtained with a Jasco J-810 spectropolarimeter. Rectangular fused quartz cells of 0.02 cm path length were used, with the sample as a 200 mM solution in methanol. The binomial method was used for smoothing the spectra. The values are expressed in terms of  $[\theta]$ , the total molar ellipticity (deg cm<sup>2</sup> dmol<sup>-1</sup>).

Restrainted molecular dynamics (MD) studies were carried out using the INSIGHT-II Discover<sup>18</sup> module on an SGI workstation. The constraints were derived from the volume integrals obtained from the ROESY spectra using a two-spin approximation and the reference distance of 1.8 Å for the geminal protons. The upper and lower bounds of the distance constraints were obtained by enhancing and reducing the derived distance by 10%.

**Boc- $\gamma$ -Caa<sub>0</sub>-OH (**10**).** A cooled (0 °C) solution of **9** (0.7 g, 1.8 mmol) in methanol (10 mL) was treated with aqueous 4 N NaOH solution (2 mL) and stirred at room temperature. After 2 h, methanol was removed. The pH was adjusted to 2–3 with aqueous 1 N HCl solution at 0 °C, and the solution was extracted with ethyl acetate (2  $\times$  10 mL). The organic layer was dried (Na<sub>2</sub>SO<sub>4</sub>) and concentrated to give **10** (0.65 g, 96%) as a white solid: mp 78–80 °C;  $[\alpha]_D = +56.7$  (c 0.25, CHCl<sub>3</sub>); IR (KBr)  $\nu$  3364, 2980, 2934, 1712, 1514, 1451, 1371,

1249, 1168, 1040 cm<sup>-1</sup>; <sup>1</sup>H NMR (CDCl<sub>3</sub>, 303 K, 500 MHz)  $\delta$  4.90 (s, 1H, C<sub>1</sub>H), 4.67 (dd, 1H,  $J = 3.7, 5.9$  Hz, C<sub>3</sub>H), 4.54 (d,  $J = 5.9$  Hz, C<sub>2</sub>H), 3.97 (m, 1H, C<sub>7</sub>H), 3.90 (m, 1H, C<sub>4</sub>H), 3.31 (s, 3H, OMe), 2.47 (m, 2H, C<sub>6</sub>H), 2.01 (m, 1H, C<sub>8</sub>H), 1.89 (m, 1H, C<sub>9</sub>H), 1.45 (s, 9H, Boc), 1.45 (s, 3H, CH<sub>3</sub>), 1.28 (s, 3H, Me); <sup>13</sup>C NMR (CDCl<sub>3</sub>, 75 MHz)  $\delta$  24.6, 26.0, 28.4, 30.7, 49.4, 54.6, 79.5, 79.8, 80.3, 85.0, 106.7, 112.7, 156.2, 178.1; HRMS (ESI)  $m/z$  calcd for C<sub>17</sub>H<sub>30</sub>NO<sub>8</sub> (M<sup>+</sup> + H) 376.1981, found 376.1967.

**Boc-L-Ala- $\gamma$ -Caa<sub>0</sub>-OMe (**13**).** A solution of **9** (0.53 g, 1.34 mmol) and TFA (1 mL) in CH<sub>2</sub>Cl<sub>2</sub> (5 mL) was stirred at room temperature for 2 h. After completion of the reaction, solvent was evaporated under reduced pressure. The resulting H- $\gamma$ -Caa<sub>0</sub>-OMe-CF<sub>3</sub>COOH (**11**) was dried under high vacuum and used as such without any further purification.

A solution of **12** (0.21 g, 1.12 mmol), HOBT (0.18 g, 1.34 mmol), and EDCI (0.25 g, 1.34 mmol) in CH<sub>2</sub>Cl<sub>2</sub> (10 mL) was stirred at 0 °C under a N<sub>2</sub> atmosphere for 15 min, treated sequentially with **11** and DIPEA (0.3 mL, 2.24 mmol), and stirred for 8 h. The reaction mixture was quenched at 0 °C with saturated NH<sub>4</sub>Cl solution (10 mL). After 10 min, the reaction mixture was diluted with CHCl<sub>3</sub> (10 mL) and then washed with 1 N HCl (10 mL), water (10 mL), aqueous saturated NaHCO<sub>3</sub> solution (10 mL), and brine (10 mL). The organic layer was dried (Na<sub>2</sub>SO<sub>4</sub>) and evaporated, and the residue was purified by column chromatography (silica gel, 60% ethyl acetate in petroleum ether) to afford **13** (0.44 g, 87%) as a white solid: mp 86–89 °C;  $[\alpha]_D = +40.9$  (c 0.4 CHCl<sub>3</sub>); IR (KBr)  $\nu$  3353, 3325, 2987, 2926, 2881, 1740, 1668, 1541, 1453, 1320, 1250, 1205, 1168, 1105, 1086 cm<sup>-1</sup>; <sup>1</sup>H NMR (CDCl<sub>3</sub>, 303 K, 500 MHz)  $\delta$  6.24 (d, 1H,  $J = 8.7$  Hz, NH-2), 5.03 (br s, 1H, NH-1), 4.87 (s, 1H, C<sub>1</sub>H), 4.66 (dd, 1H,  $J = 3.6, 6.2$  Hz, C<sub>3</sub>H), 4.53 (d, 1H,  $J = 6.2$  Hz, C<sub>2</sub>H), 4.29 (m, 1H, C<sub>7</sub>H), 4.11 (m, 1H, C<sub>6</sub>H), 3.92 (dd, 1H,  $J = 3.6, 7.5$  Hz, C<sub>4</sub>H), 3.66 (s, 3H, COOMe), 3.29 (s, 3H, OMe), 2.40 (m, 2H, C<sub>6</sub>H), 2.10 (m, 1H, C<sub>8</sub>H), 1.88 (m, 1H, C<sub>9</sub>H), 1.46 (s, 3H, Me), 1.44 (s, 9H, Boc), 1.35 (d,  $J = 7.0$  Hz, CH<sub>3</sub>), 1.28 (s, 3H, Me); <sup>13</sup>C NMR (CDCl<sub>3</sub>, 75 MHz)  $\delta$  18.1, 24.8, 26.1, 26.8, 28.3, 30.5, 48.7, 50.4, 51.5, 54.6, 79.8, 80.3, 85.1, 106.8, 112.8, 155.5, 172.4, 173.9; HRMS (ESI)  $m/z$  calcd for C<sub>21</sub>H<sub>37</sub>N<sub>2</sub>O<sub>9</sub> (M<sup>+</sup> + H) 461.2499, found 461.2462.

**Boc-L-Ala- $\gamma$ -Caa<sub>0</sub>-OH (**14**).** As described for the synthesis of **10**, a solution of **13** (0.15 g, 0.33 mmol) gave **14** (0.14 g, 96%) as a white solid: mp 69–72 °C;  $[\alpha]_D = +44.6$  (c 0.25, CHCl<sub>3</sub>); IR (KBr)  $\nu$  3331, 2983, 2936, 1709, 1527, 1453, 1374, 1252, 1165, 1093 cm<sup>-1</sup>; <sup>1</sup>H NMR (CDCl<sub>3</sub>, 303 K, 500 MHz)  $\delta$  6.60 (d, 1H,  $J = 9.3$  Hz, NH-2), 5.34 (br s, 1H, NH-1), 4.87 (s, 1H, C<sub>1</sub>H), 4.65 (dd, 1H,  $J = 3.5, 5.9$  Hz, C<sub>3</sub>H), 4.54 (d, 1H,  $J = 5.9$  Hz, C<sub>2</sub>H), 4.38 (m, 1H, C<sub>7</sub>H), 4.21 (m, 1H, C<sub>6</sub>H), 3.91 (dd, 1H,  $J = 3.5, 7.9$  Hz, C<sub>4</sub>H), 3.27 (s, 3H, OMe), 2.41 (m, 2H, C<sub>6</sub>H), 2.08 (m, 1H, C<sub>8</sub>H), 1.89 (m, 1H, C<sub>9</sub>H), 1.47 (s, 3H, Me), 1.45 (s, 9H, Boc), 1.35 (d,  $J = 6.8$  Hz, CH<sub>3</sub>), 1.28 (s, 3H, Me); <sup>13</sup>C NMR (CDCl<sub>3</sub>, 75 MHz)  $\delta$  18.7, 24.9, 26.1, 26.6, 28.3, 30.8, 48.9, 50.2, 54.5, 79.6, 80.1, 80.7, 85.2, 106.9, 112.9, 155.8, 173.1; HRMS (ESI)  $m/z$  calcd for C<sub>20</sub>H<sub>35</sub>N<sub>2</sub>O<sub>9</sub> (M<sup>+</sup> + H) 447.2342, found 447.2336.

**Boc-L-Ala- $\gamma$ -Caa<sub>0</sub>-L-Ala-OMe (**1**).** According to the procedure described for **13**, a mixture of **14** (0.2 g, 0.45 mmol), HOBT (0.06 g, 0.5 mmol), and EDCI (0.09 g, 0.5 mmol) in CH<sub>2</sub>Cl<sub>2</sub> (15 mL) was stirred at 0 °C for 15 min and then treated with **15** (0.07 g, 0.5 mmol) and DIPEA (0.1 mL, 0.9 mmol) under a N<sub>2</sub> atmosphere for 8 h. Workup and purification by column chromatography (silica gel, 80% ethyl acetate in petroleum ether) afforded **1** (0.17 g, 71%) as a white solid: mp 94–97 °C;  $[\alpha]_D = +39.1$  (c 0.55, CHCl<sub>3</sub>); IR (KBr)  $\nu$  3365, 3274, 3076, 2986, 2941, 1739, 1708, 1661, 1560, 1514, 1454, 1369, 1298, 1250, 1210, 1111, 1065, 1014, 973, 761, 695, 651 cm<sup>-1</sup>; <sup>1</sup>H NMR (CDCl<sub>3</sub>, 303 K, 500 MHz)  $\delta$  7.36 (d, 1H,  $J = 6.5$  Hz, NH-3), 6.62 (d, 1H,  $J = 8.8$  Hz, NH-2), 5.09 (d, 1H,  $J = 7.3$  Hz, NH-1), 4.86 (s, 1H, C<sub>1</sub>H-2), 4.69 (dd, 1H,  $J = 3.5, 5.8$  Hz, C<sub>3</sub>H-2), 4.53 (m, 1H, C<sub>6</sub>H-3), 4.52 (d, 1H,  $J = 5.8$  Hz, C<sub>2</sub>H-2), 4.34 (m, 1H, C<sub>7</sub>H-2), 4.11 (m, 1H, H-Ala1), 3.85 (dd, 1H,  $J = 3.5, 8.6$  Hz, C<sub>4</sub>H-2), 3.75 (s, 3H, COOMe), 3.29 (s, 3H, OMe), 2.22 (m, 1H, C<sub>6</sub>H-2), 2.16 (m, 1H, C<sub>6</sub>H-2), 1.90

(18) Discover, Version 2.98; Biosym Molecular Simulations: San Diego, CA, 1995.









and DIPEA (0.06 mL, 0.32 mmol) under a N<sub>2</sub> atmosphere for 8 h. Workup and purification by column chromatography (silica gel, 4% MeOH in CHCl<sub>3</sub>) furnished **8** (0.12 g, 44.9%) as a white solid: mp 160–165 °C; [α]<sub>D</sub> = –50.33 (c, 0.5, CHCl<sub>3</sub>); IR (KBr) ν 3297, 2985, 2931, 1660, 1541, 1378, 1168, 1081, 1022, 855 cm<sup>-1</sup>; <sup>1</sup>H NMR (CDCl<sub>3</sub>, 288 K, 600 MHz) δ 7.68 (d, 1H, *J* = 8.6 Hz, NH-5), 7.40 (d, 1H, *J* = 9.6 Hz, NH-6), 7.34 (d, 1H, *J* = 9.0 Hz, NH-4), 7.17 (d, 1H, *J* = 9.2 Hz, NH-3), 6.39 (d, 1H, *J* = 8.2 Hz, NH-2), 6.03 (d, 1H, *J* = 9.7 Hz, NH-1), 6.02 (d, 1H, *J* = 3.8 Hz, C<sub>1</sub>H-6), 5.90 (d, 1H, *J* = 3.8 Hz, C<sub>1</sub>H-5), 5.88 (d, 2H, *J* = 3.8 Hz, C<sub>1</sub>H-1, 3), 5.85 (d, 1H, *J* = 3.8 Hz, C<sub>1</sub>H-4), 5.84 (d, 1H, *J* = 3.8 Hz, C<sub>1</sub>H-2), 4.62 (d, 1H, *J* = 3.8 Hz, C<sub>2</sub>H-2), 4.61 (d, 1H, *J* = 3.8 Hz, C<sub>2</sub>H-4), 4.60 (d, 1H, *J* = 3.8 Hz, C<sub>2</sub>H-5), 4.59 (d, 1H, *J* = 3.8 Hz, C<sub>2</sub>H-1), 4.58 (m, 1H, C<sub>β</sub>H-3), 4.56 (d, 2H, *J* = 3.8 Hz, C<sub>2</sub>H-3, 6), 4.46 (m, 1H, C<sub>β</sub>H-5), 4.35 (m, 1H, C<sub>γ</sub>H-6), 4.30 (m, 1H, C<sub>β</sub>H-1), 4.28 (m, 1H, C<sub>γ</sub>H-4), 4.26 (m, 1H, C<sub>4</sub>H-5), 4.26 (dd, 1H, *J* = 2.6, 3.2 Hz, C<sub>4</sub>H-2), 4.24 (m, 1H, C<sub>γ</sub>H-2), 4.16 (dd, 1H, *J* = 3.2, 9.9 Hz, C<sub>4</sub>H-3), 4.08 (dd, 1H, *J* = 3.2, 7.8 Hz, C<sub>4</sub>H-4), 4.06 (dd, 1H, *J* = 3.2, 8.0 Hz, C<sub>4</sub>H-6), 4.05 (dd, 1H, *J* = 3.2, 9.6 Hz, C<sub>4</sub>H-1), 3.93 (d, 1H, *J* = 3.2 Hz, C<sub>3</sub>H-5), 3.88 (d, 1H, *J* = 3.2 Hz, C<sub>3</sub>H-3), 3.83 (d, 1H, *J* = 3.2 Hz, C<sub>3</sub>H-2), 3.71 (d, 1H, *J* = 3.2 Hz, C<sub>3</sub>H-1), 3.68 (d, 1H, *J* = 3.2 Hz, C<sub>3</sub>H-4), 3.65 (d, 1H, *J* = 3.2 Hz, C<sub>3</sub>H-6), 3.65 (s, 3H, COOMe), 3.41 (s, 3H, OMe-1), 3.40 (s, 3H, OMe-2), 3.39 (s, 3H, OMe-4), 3.38 (s, 6H, OMe-3, 6), 3.35 (s, 3H, OMe-5), 2.52 (m, 1H, C<sub>α</sub>H-3), 2.50 (m, 1H, C<sub>α</sub>H-6), 2.49 (m, 1H, C<sub>α</sub>H-5), 2.43

(m, 1H, C<sub>α</sub>H-6), 2.41 (m, 1H, C<sub>α</sub>H-1), 2.38 (m, 1H, C<sub>α</sub>H-3), 2.28 (m, 2H, C<sub>α</sub>H, C<sub>α</sub>H-4), 2.27 (m, 2H, C<sub>α</sub>H, C<sub>α</sub>H-2), 2.26 (m, 1H, C<sub>α</sub>H-1), 2.03 (m, 1H, C<sub>β</sub>H-2), 1.92 (m, 1H, C<sub>β</sub>H-4), 1.83 (m, 1H, C<sub>β</sub>H-6), 1.78 (m, 1H, C<sub>β</sub>H-6), 1.72 (m, 1H, C<sub>β</sub>H-2), 1.68 (m, 1H, C<sub>β</sub>H-4), 1.50 (s, 6H, Me), 1.46 (s, 9H, Boc), 1.44 (s, 3H, Me), 1.43 (s, 6H, Me), 1.31 (s, 3H, Me), 1.30 (s, 6H, Me), 1.29 (s, 3H, Me), 1.25 (s, 9H, Me); <sup>13</sup>C NMR (CDCl<sub>3</sub>, 150 MHz) δ 26.0, 26.1, 26.6 (4), 26.8, 28.4 (3), 29.7 (3), 30.3, 30.9, 38.7, 39.6, 39.7, 40.0, 40.7, 45.4, 46.2, 46.3, 46.4, 46.5, 46.7, 47.2, 47.3, 47.4, 47.6, 51.6, 51.7, 57.1, 57.2, 57.3, 57.4, 57.5, 57.8, 57.9, 79.2, 79.7, 80.8, 81.1, 81.2, 81.3, 81.6, 83.1, 83.2, 83.3, 83.5, 83.8, 84.1, 84.2, 85.4, 96.0, 104.5, 104.6, 104.7, 104.8, 104.9, 111.1, 111.3, 111.4, 111.6, 111.9, 156.0, 170.0, 170.2, 170.5, 170.6, 170.7, 171.0, 172.2, 172.7, 173.9; HRMS (ESI) *m/z* calcd for C<sub>75</sub>H<sub>120</sub>N<sub>6</sub>O<sub>33</sub> (M<sup>+</sup> + Na) 1655.7794, found 1655.7763.

**Acknowledgment.** The authors are thankful to Prof. Hofmann, University of Leipzig, Germany for fruitful discussions. V.B.J., P.J., K.N., and V.S. are thankful to CSIR, New Delhi, for financial support.

**Supporting Information Available:** NMR/CD spectra and details of the MD calculations. This material is available free of charge via the Internet at <http://pubs.acs.org>.

JA064875A